Contents lists available at SciOpen

Food Science and Human Wellness

journal homepage: https://www.sciopen.com/journal/2097-0765

China Food Publishing Co.

Phlorizin alleviates mastitis and preserves the blood-milk barrier by metabolizing into phloretin

Xin Ran[1], Kefei Li[1], Juxiong Liu[1], Xiaoxuan Wang, Wenjin Guo, Guiqiu Hu, Shoupeng Fu*

State Key Laboratory for Diagnosis and Treatment of Severe Zoonotic Infectious Diseases, Key Laboratory for Zoonosis Research of the Ministry of Education, Institute of Zoonosis, College of Veterinary Medicine, Jilin University, Changchun 130062, China

ARTICLE INFO

Article history:
Received 29 September 2023
Received in revised form 6 November 2023
Accepted 8 December 2023

Keywords:
Phlorizin
Phloretin
Mastitis
Blood-milk barrier
Pyroptosis
Intestinal flora

ABSTRACT

Mastitis is a common disease that affects women during lactation, posing a threat to the health of both mothers and infants. Recent studies have shown that insufficient nutrient intake increase the risk of mastitis. Phlorizin (PHZ) is one of the nutrients present in apples. This study uses lipopolysaccharide (LPS)-induced mastitis mice and LPS + ATP-stimulated mouse mammary epithelial cells (mMECs) as research objects to explore the effect and mechanism of PHZ on mastitis. Different from *in vitro* beliefs, our findings demonstrated that PHZ significantly reduced inflammation and protected the blood-milk barrier (BMB) *in vivo*. Additionally, we observed that oral administration of PHZ regulated the intestinal flora and exhibited prebiotic functions. However, the anti-inflammatory effect of PHZ was not solely dependent on the intestinal flora, as antibiotic disruption of the intestinal flora does not completely abolish the improvement of mastitis by PHZ. Further mechanistic research revealed that the anti-inflammatory properties of PHZ were attributed to its metabolism into phloretin (PHT). Moreover, our results demonstrated that PHT reduced inflammation and protected the BMB by promoting autophagy to prevent the pyroptosis of mMECs. This study provides a theoretical basis for reducing inflammation in lactating women by consuming fruits, such as apples, that contain PHZ.

1. Introduction

Mastitis, a common disease among lactating women, often occurs within the first month after delivery. Primiparas are at a significantly higher risk of developing mastitis compared to women who have given birth multiple times[1]. Infections caused by *Escherichia coli* and *Staphylococcus aureus* are important factors contributing to mastitis. Untreated mastitis can progress to suppurative mastitis and increase the chances of sepsis[2-3]. Mastitis not only poses a threat to women's health but also hampers breastfeeding, affecting the nutritional intake and composition of infants during their growth period[4]. Consequently, preventing and treating mastitis are crucial for maternal and child health[5].

Mammary epithelial cells, which are plentiful in the mammary gland, are important in both regulating inflammation through immunological activity and building the blood-milk barrier (BMB), thereby maintaining the homeostasis of the mammary internal environment[6]. Pathogenic bacteria stimulate mammary epithelial cells, causing them to pyroptosis and release a significant number of intracellular proinflammatory factors, creating an inflammatory cascade reaction[7-8]. Moreover, the death of mammary epithelial cells disrupts the integrity of the BMB, reducing the migration threshold of immune cells, including macrophages, across the BMB. This induces immune cell aggregation in the mammary gland and promotes mastitis intensification[6,9]. Thus, inhibiting pyroptosis of mammary epithelial cells may help alleviate mastitis.

[1] These authors contributed equally to this work.
* Corresponding author at: College of Veterinary Medicine, Jilin University, Changchun 130062, China.
E-mail address: fushoupeng@jlu.edu.cn (S.P. Fu)
Peer review under responsibility of Beijing Academy of Food Sciences.

SciOpen Publishing services by Tsinghua University Press

http://doi.org/10.26599/FSHW.2024.9250147

Recent studies indicate that lactating women with insufficient nutrient intake have a higher risk of developing mastitis[10]. Apples have long been known to have a substantial favorable impact on preserving body health, as evident in the saying "an apple a day keeps the doctor away"[11]. The high nutritional value of apples was previously attributed to their high vitamin content, such as vitamins C and E[12]. Later, the discovery of the nutrient phlorizin (PHZ) in apples validated its efficacy in alleviating multiple diseases[13-14]. PHZ, a dihydrochalcone compound, has been extensively studied for its potential to improve obesity and type 2 diabetes owing to its competitive inhibition activity of sodium-glucose cotransporter 2[15-16]. Moreover, the anti-inflammatory effects of PHZ also have been reported[17-18].

Therefore, the question arises: can PHZ, a nutrient present in apples, alleviate mastitis when administered orally? Using the lipopolysaccharide (LPS)-induced mice mastitis model, we sought to investigate the impact of PHZ on mastitis and its underlying mechanism in order to answer this question. This study provided theoretical support for consuming PHZ-containing fruits, such apples, during lactation in order to reduce inflammation in the body.

2. Materials and methods

2.1 Animal and experimental design

In this study, the specific pathogen-free BALB/c mice (7 weeks old) were obtained from Liaoning Changsheng Biotechnology Co., Ltd. (China). After 1 week of acclimation to the environment, the mice were placed in breeding cages with 1 male and 2 females, and they had *ad libitum* access to food and water with 12-h light and dark cycles. Pregnancy was determined *via* vaginal plug observation, and pregnant mice were then transferred to new cages for the experiments. All mouse experiments strictly followed the guidelines of the Institutional Animal Care and Use Committee of Jilin University (Protocol No. SY202309041).

The *in vivo* experiment was divided into 2 key parts: a PHZ supplementation experiment and an antibiotic treatment experiment. For the PHZ supplementation experiment, standard product of PHZ was purchased from Shanghai Yuanye Bio-Technology Co., Ltd. (HPLC ≥ 98%). The PHZ was dissolved in sterile saline for oral administration. A total of 24 pregnant female mice at 1 week of gestation were randomly divided into 4 groups, each containing 6 mice. (1) NT group: normal feeding for 3 weeks; (2) PHZ group: gavage of PHZ (80 mg/(kg · day)) for 3 weeks; (3) LPS group: a mastitis mouse model was established after 3 weeks of normal feeding; (4) PHZ + LPS group: a mastitis mouse model was established by gavage of PHZ (80 mg/(kg · day)) for 3 weeks. In the antibiotic treatment experiment, an antibiotic cocktail (ABX) was prepared by dissolving 1 g ampicillin, 1 g metronidazole, 1 g neomycin, and 0.5 g vancomycin in 1 L drinking water. A total of 18 newly pregnant female mice were randomly divided into 3 groups, each containing 6 mice. (1) ABX group: normal feeding and supplemented with ABX for 4 weeks; (2) ABX + LPS group: a mastitis mouse model was established after normal feeding and ABX supplementation for 4 weeks; (3) ABX + LPS + PHZ group: after 4 weeks of ABX supplementation, the mice received gavage of PHZ (80 mg/(kg · day)) for 3 weeks to establish the mastitis mouse model. The mastitis mouse model was constructed by injecting LPS into the mammary ducts on the seventh day after delivery.

2.2 Construction of mastitis mouse model

One week after delivery, the female mice were separated from their offspring and anesthetized with pentobarbital sodium. They were placed supine on a mouse fixation plate, and the fourth pair of nipples was disinfected with 75% ethanol. Surgical scissors were used to remove 1 mm of the nipple, and 50 μL of LPS (2 μg/mL) was injected into the mammary ducts using an anatomical microscope and a 34 G needle. The control group received PBS injection into their mammary ducts after anesthesia. After 24 h of mastitis model construction, mammary tissues from all mice were collected for further analyses.

2.3 Hematoxylin and eosin (H&E) staining

Mouse mammary tissue slices were dewaxed with xylene, hydrated with different concentrations of ethanol, stained with hematoxylin, rinsed with water, and placed in 80% and 90% ethanol. Subsequently, the slices were stained with eosin, dehydrated with various concentrations of ethanol, sealed in xylene, and mounted with neutral resin. Based on a prior study, the mammary injury score was determined[19].

2.4 Immunofluorescence

After removing the paraffin from the mammary tissue slices, they were hydrated with different concentrations of ethanol. The slices were placed in a citrate buffer and heated 2–3 times to complete antigen repair. The slices were sealed with 5% donkey serum for 2 h after they had cooled. The first antibody was diluted with 5% donkey serum and used to incubate the slices overnight at 4 ℃. The slices were then incubated with the secondary antibody diluted in PBS for 1 h. The nucleus was stained with DAPI, and a fluorescence microscope was used to observe and record the target protein. The mMEC slides were fixed using the immunostaining fixative solution and sealed with donkey serum. Subsequent steps were the same as those for the immunofluorescence of tissue slices.

2.5 Myeloperoxidase (MPO) analysis

Mouse mammary tissue was treated with 50 mmol/L of *N*-2-hydroxyethylpiperazine-*N*-2-ethane sulfonic acid (HEPES) solution at a ratio of 1:5 000. An automatic grinder was used to grind tissues, followed by centrifugation (10 000 × *g*, 8 min, 4 ℃) to obtain the supernatant for enzyme-linked immunosorbent assay (ELISA) samples. To the EP tube containing the precipitate, 0.5% cetyltrimethylammonium chloride (CTAC) was added in an amount equal to the volume of HEPES, followed by grinding and centrifugation (10 000 × *g*, 8 min, 4 ℃). The supernatant was collected, and a substrate chromogenic solution containing tetramethylbenzidine (TMB), H_2O_2, and resorcinol was prepared and added to the supernatant to detect the MPO content in the samples.

2.6 ELISA

An ELISA kit (Biolegend, USA) was used to detect the content of pro-inflammatory factors (interleukin-1β (IL-1β), interleukin-6 (IL-6),

and tumor necrosis factor-α (TNF-α) in the mammary tissue of mice. The sensitivity of kits of IL-1β, IL-6, and TNF-α respectively are 0.5, 2.0, and 4.0 pg/mL. The standard range of kits of IL-1β, IL-6, and TNF-α respectively are 2.0–125.0, 7.8–500.0, and 7.8–500.0 pg/mL.

2.7 16S rRNA sequencing of intestinal flora

The total DNA in each sample was extracted. Primers were designed according to the conserved region, and sequencing connectors were added to the end of the primers for PCR amplification. The products were then purified, quantified, and homogenized to form sequencing libraries. Based on the Illumina Hiseq 2500 platform (Biomaker Technology, China), a small fragment library was constructed using the paired-end method for sequencing bacterial genes. The high-quality sequences were clustered, denoised, and divided into operational taxonomic units (OTUs). Taxonomic analysis was performed for each sample at each classification level based on the OTU analysis. Community structure maps and species clustering heat maps of each sample at the taxonomic level of phyla, class, order, family, and genus were obtained. Species diversity was analyzed using *α*-diversity, and the Ace, Chao1, Shannon, and Simpson indices of each sample were calculated. Additionally, sample dilution curves and grade abundance curves were drawn. *β*-Diversity analysis was used to compare the size of differences in species diversity, such as community composition and structure, between different samples. Based on the distance matrix, the unweighted pair group method with arithmetic mean (UPGMA) tree, non-metric multidimensional scaling (NMDS) analysis graphs, sample clustering heat maps, principal component analysis (PCA), and principal coordinate analysis (PCoA) graphs were obtained.

2.8 Detection short-chain fatty acids (SCFAs) in feces

The mouse feces were mixed with phosphoric acid, isohexic acid, and ether and subsequently centrifuged (12 000 × *g*, 8 min, 4 ℃). The supernatant was collected for the detection of SCFAs. Specific gas (Trace 1300, Thermo) and mass (ISQ 7000, Thermo) chromatography methods were used for the detection, as described previously[20].

2.9 Western blotting analysis

NP40 (Beyotime, China) was used to lyse cells or mammary tissue. The protein concentration was determined using the BCA kit (Thermo Scientific, USA), and all samples were grouped based on their protein content, which was standardized using the protein concentration. Subsequently, 12% sodium dodecyl sulfate-polyacrylamide gel electrophoresis (SDS-PAGE) was performed. After the protein was transferred to a PVDF membrane, it was incubated at 4 ℃ with the primary antibody overnight, followed by incubation with the secondary antibody at room temperature for 1 h. The information on antibodies used in this study is listed in Table S1. Finally, the electrochemiluminescence detection kit (Beyotime, Wuhan, China) was used to obtain the visual results of protein bands.

2.10 Reverse transcription quantitative real-time polymerase chain reaction (qRT-PCR)

The total mRNA of mMECs was extracted using TRIzol (Invitrogen, USA). The process of RNA qRT-PCR were performed as previously reported[19]. The primer sequences are listed in Table S2.

2.11 Cell viability test

The cell counting kit-8 (CCK-8; Saint-Bio, Shanghai, China) was used to detect the cell viability of mMECs. After inoculating mMECs into 96-well plates, they were treated with PHZ, phloretin (PHT), or LPS and adenosine triphosphate (ATP) successively. The CCK-8 reagent was added to each well for 4 h, and the detection results were obtained using an enzyme labeler. The Annexin V-FITC apoptosis detection kit (Beyotime, China) was used to detect pyroptosis. Following the respective treatments, the cells were incubated with PI and Annexin V-FITC reagents, and flow cytometry was used to analyze cell pyroptosis. For further details, please refer to the operating instructions provided with the kit.

2.12 Determination of PHZ and PHT levels in the serum

A 100 μL mouse blood sample was taken, and 1 mL ethyl acetate was added to the samples and mixed by shaking. The test tube was then centrifuged at 10 000 × *g* and 4 ℃ for 10 min. The upper organic phase was transferred to a new 1.5 mL tube and evaporated to dryness under a stream of nitrogen. The precipitate in the 1.5 mL tube was dissolved using 100 μL methanol. The methanol solution was centrifuged (10 000 × *g*, 5 min, 4 ℃), and the supernatant was collected for detection. An established HPLC method was used to quantify the contents of PHZ and PHT[21].

2.13 Autophagy flux analysis

The mMECs were transferred to a 24-well plate and transfected with mRFP-GFP-LC3 double standard plasmid (0.8 μg/well) and Lipofectamine 2000 (Invitrogen, USA) for 48 h. After the mMECs were treated according to the experimental conditions, they were washed with PBS and then fixed with immunostaining fixative (Beyotime, China) at room temperature for 20 min. Subsequently, the mMECs were sealed using a tablet containing DAPI. Laser confocal microscopy was used to observe and record autophagy flux. Finally, the assessment of autophagy flux involved counting the number of yellow dots (representing autophagosomes) and red dots (representing autolysosomes).

2.14 Molecular modeling

The structure of PHT was downloaded from the PubChem database (https://pubchem.ncbi.nlm.nih.gov/), and the 2D structure model was converted to a 3D model. The 3D structure of the AKT protein was downloaded from the RCSB Protein Data Bank (https://www.rcsb.org) and used as the protein for this project. The compound was virtually docked with the protein target using Autodock 4.2.6. The docking results were visually analyzed using PyMOL 2.2.0 and Discovery Studio Client v19.1.0.

2.15 Data analysis

GraphPad Prism 8 software was used to perform statistical analysis. All data are presented as mean ± standard deviation (SD), and one of the 3 independent and repeated experiments was selected as the representative data. One-way analysis of variance (ANOVA) and Tukey's post-hoc test was used to analyze the significance of differences between multiple groups. *T*-test was used to verify the statistical difference between the two groups. Results at $P < 0.05$ were considered statistically significant, and those at $P < 0.01$ were considered extremely significant.

3. Results

3.1 Oral administration of PHZ ameliorates LPS-induced mastitis in mice.

To investigate the potential effects of PHZ on mastitis, mice administered PHZ orally before establishing the mouse mastitis model. Visual observation revealed that LPS stimulation remarkably induced redness and swelling in the mammary tissue, and PHZ treatment significantly alleviated these symptoms (Fig. 1A). Histological analysis using H&E staining further validated that PHZ significantly reduced the thickening of mammary acinar walls and

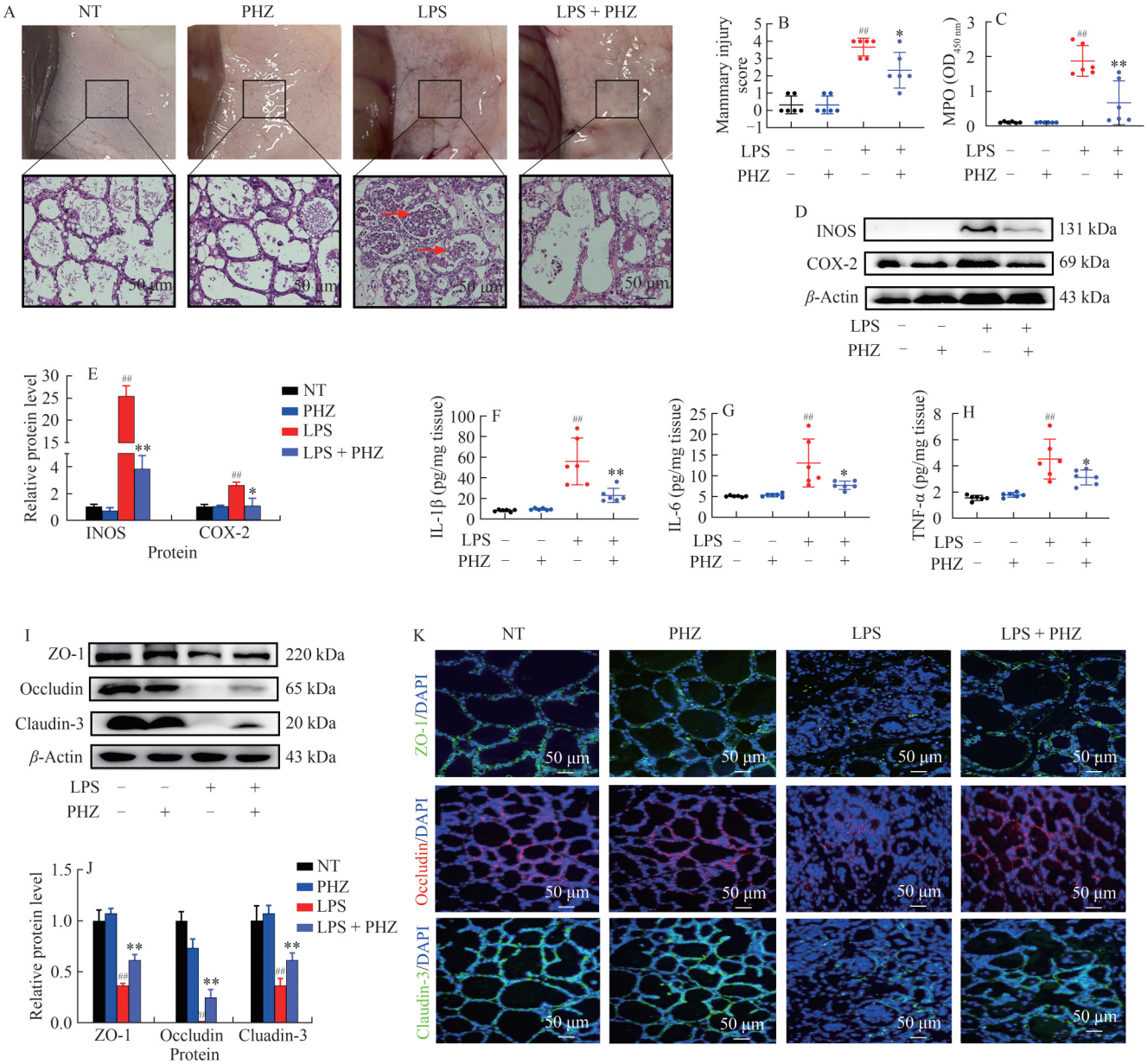

Fig. 1 Oral administration of PHZ ameliorates LPS-induced mastitis in mice. (A) Representative photographs and H&E staining images of mouse mammary glands. The red arrows indicate inflammatory cell infiltration. Scale bar: 50 μm. (B) Mammary injury score based on H&E staining. (C) MPO levels in mammary glands. (D and E) Representative bands and relative protein levels of proinflammatory enzymes (INOS and COX-2). *β*-Actin was used as the internal control to obtain the relative protein intensity. (F-H) Contents of proinflammatory factors IL-1β (F), IL-6 (G), and TNF-α (H) in mouse mammary tissue. (I and J) Representative bands and relative protein levels of TJs (ZO-1, Occludin, and Claudin-3). (K) Representative images of the immunofluorescence of TJs (ZO-1, Occludin, and Claudin-3). Scale bar: 50 μm. Data are presented as mean ± SD ($n = 6$). $^{\#\#}P < 0.01$ *vs*. no-treatment (NT) group; $^{*}P < 0.05$ or $^{**}P < 0.01$ *vs*. LPS group.

infiltration of inflammatory cells in mammary acini caused by LPS stimulation (Fig. 1A). Subsequently, the evaluation of mammary injury score and MPO levels demonstrated that PHZ alleviated the symptoms of mastitis and reduced inflammatory cell infiltration in mammary tissue (Figs. 1B and C). Pro-inflammatory mediators play a pivotal role in exacerbating inflammation. The analysis of pro-inflammatory factors in mammary tissue revealed that LPS stimulation significantly increased the secretion of IL-1β, IL-6, and TNF-α, whereas PHZ treatment effectively reduced their secretion (Figs. 1F-H). The results of pro-inflammatory enzymes, inducible nitric oxide synthase (INOS) and cyclooxygenase-2 (COX-2) displayed a similar pattern (Figs. 1D and E). Mammary inflammation often results in the destruction of the BMB, further aggravating the inflammatory response. Therefore, we investigated the integrity of the BMB and observed that LPS stimulation reduced the expression of the tight junction proteins (TJs) ZO-1, Occludin, and Claudin-3, whereas oral administration of PHZ significantly increased their expression (Figs. 1I-K). Collectively, these results indicated that oral administration of PHZ alleviates LPS-induced mammary inflammation and disruption of the BMB in mastitis mice.

3.2 Oral administration of PHZ inhibits LPS-induced pyroptosis in mouse mammary tissue.

Numerous studies have confirmed the association of mastitis with pyroptosis, which exacerbates inflammation and tissue damage. Firstly, the results showed that PHZ significantly reduced the expression and activation of gasdermin D (GSDMD), which was enhanced by LPS stimulation (Figs. 2A and B). The immunohistochemistry results of N-GSDMD in mammary tissue showed that PHZ significantly reduced the production of N-GSDMD (Fig. 2C). Moreover, the expression of N-GSDMD was notably concentrated in mammary epithelial cells, indicating that PHZ reduced the occurrence of pyroptosis in these cells during mastitis. The NF-κB signaling pathway and NOD-like receptor thermal protein domain associated protein 3 (NLRP3) inflammasome promote pyroptosis by regulating the expression and activation of GSDMD, respectively. Our results indicated that PHZ reduced the activation of the NF-κB signaling pathway and NLRP3 inflammasome in mouse mammary tissue (Figs. 2D-G). These findings suggest that PHZ suppresses pyroptosis in mammary tissue by inhibiting the activation of the NF-κB signaling pathway and NLRP3 inflammasome.

3.3 Lack of anti-inflammatory effect of PHZ in LPS + ATP-stimulated mMECs.

We conducted *in vitro* experiments using mMECs to validate the anti-inflammatory effects of PHZ. Initial cell viability tests revealed that concentrations of PHZ below 200 μmol/L did not affect mMECs (Fig. S1A). Consequently, we used PHZ at 25, 50, and 100 μmol/L were used for subsequent experiments. When mMECs were stimulated with LPS + ATP, the expression of *IL-1β*, *IL-6*, *TNF-α*, *INOS*, and *COX-2* was significantly increased, whereas PHZ did not affect the high expression of these pro-inflammatory mediators (Figs. 3A and S1B). Based on these results, we selected 100 μmol/L PHZ for further analysis. Our investigations into the NF-κB signaling pathway revealed that PHZ had no significant effect on their activation (Figs. 3B and C). Moreover, PHZ did not affect the nuclear translocation of NF-κB p65 in LPS + ATP-stimulated mMECs (Fig. 3D). The detection of TJs in mMECs showed that PHZ did not alleviate the loss of TJs caused by LPS + ATP (Figs. 3E and F and H). Additionally, PHZ did not mitigate the reduction in cell activity of

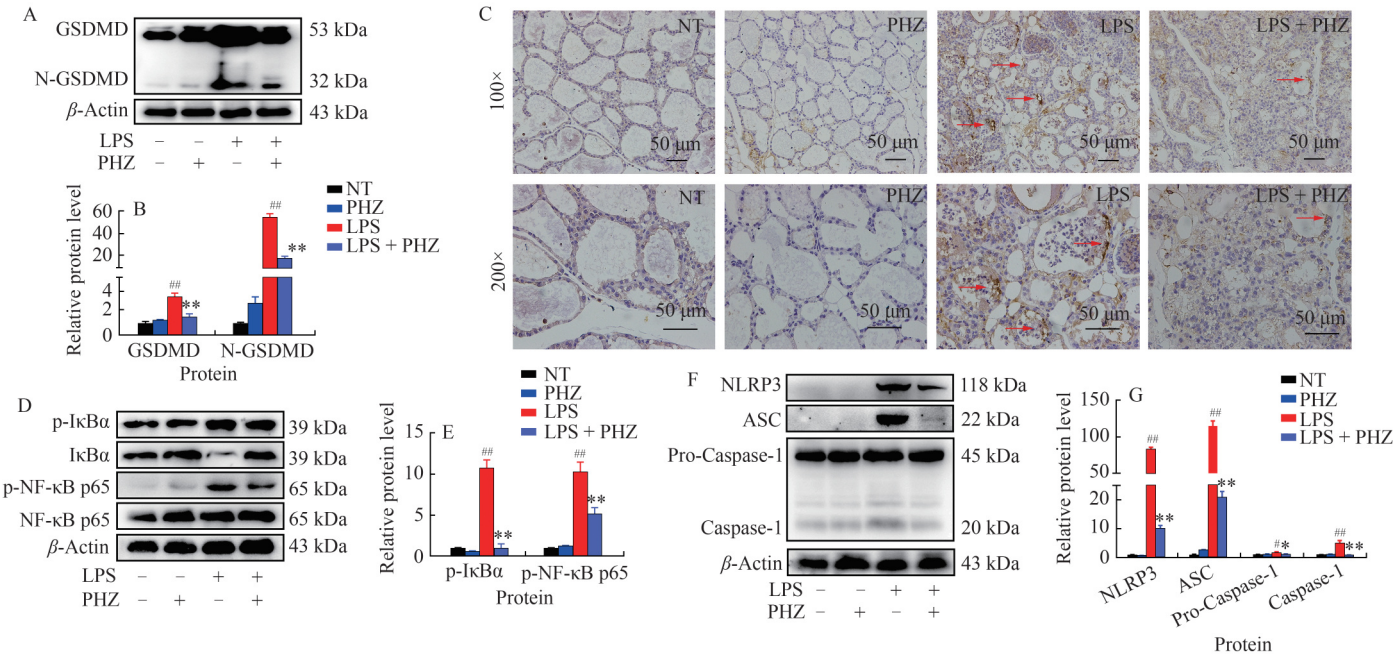

Fig. 2 Oral administration of PHZ inhibits LPS-induced pyroptosis in mouse mammary tissue. (A, B) Representative bands and relative protein levels of GSDMD and N-GSDMD. (C) Immunohistochemistry of N-GSDMD in mouse mammary gland. Scale bar: 50 μm. (D) Representative bands of p-IκBα, IκBα, p-NF-κB p65, and NF-κB p65. (E) Relative protein levels of p-IκBα and p-NF-κB p65. (F and G) Representative bands and relative protein levels of NLRP3, ASC, pro-Caspase-1, and Caspase-1. Data are presented as mean ± SD ($n = 3$). $^{\#\#}P < 0.01$ *vs*. NT group; $^{*}P < 0.05$ or $^{**}P < 0.01$ *vs*. LPS group.

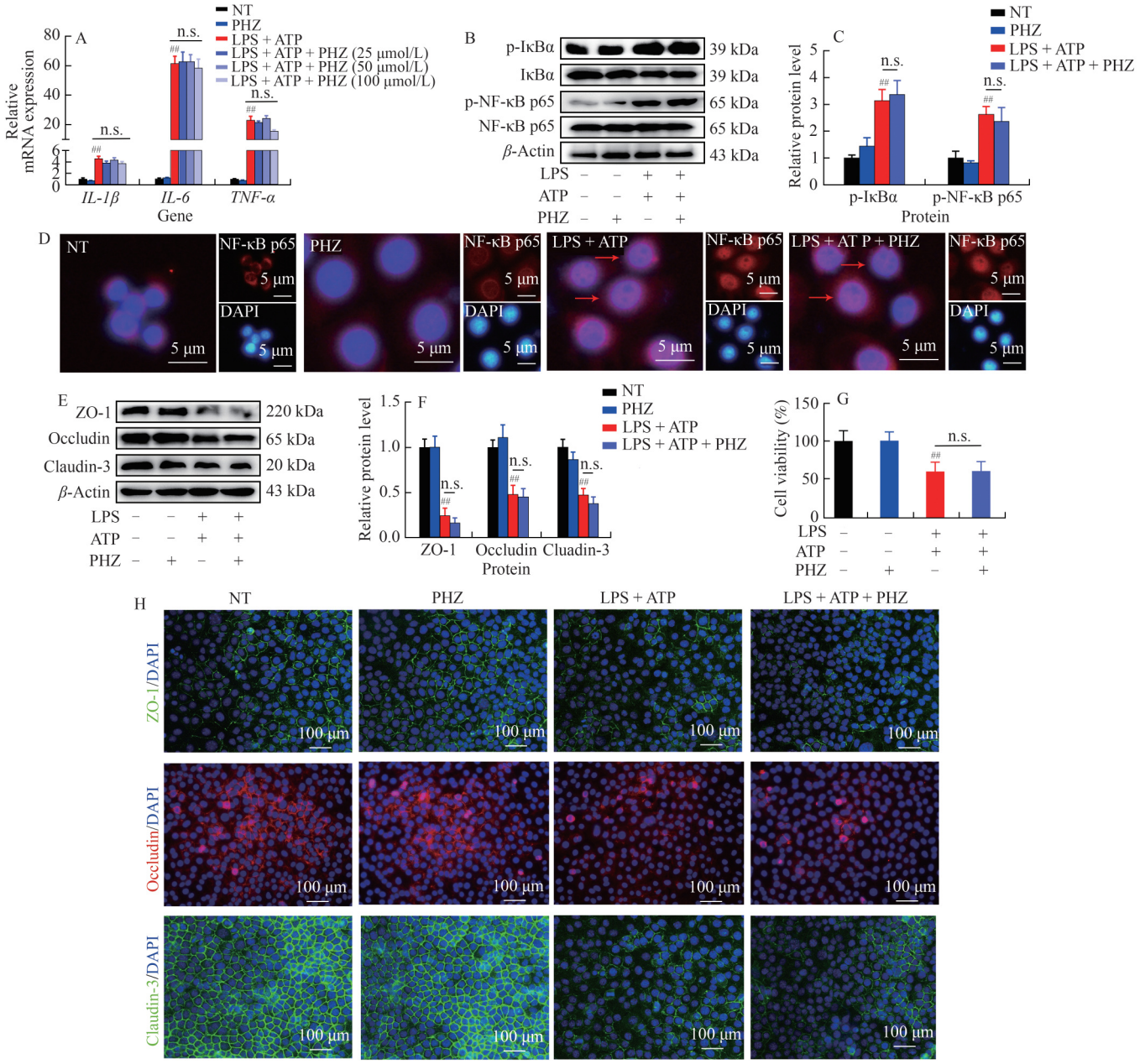

Fig. 3 Lack of anti-inflammatory effect of PHZ in LPS + ATP-stimulated mMECs. The mMECs were treated with PHZ for 1 h, followed by stimulation with LPS (1 μg/mL) for 4 or 24 h, and ATP (5 mmol/L) co-stimulation was introduced either 30 or 90 min before the completion of LPS stimulation. (A) Relative mRNA expression of pro-inflammatory factors. (B) Representative bands of p-IκBα, IκBα, p-NF-κB p65, and NF-κB p65. (C) Relative protein levels of p-IκBα and p-NF-κB p65. (D) Nuclear translocation of NF-κB p65 of mMECs under different treatments. Scale bar: 5 μm. (E) Representative bands of TJs. (F) Representative relative protein levels of TJs. (G) Cell viability of mMECs under different treatments. (H) Representative images of the immunofluorescence of TJs. Scale bar: 100 μm. Data are presented as mean ± SD ($n = 3$). $^{\#\#}P < 0.01$ *vs.* NT group; n.s. not significant.

mMECs caused by LPS + ATP stimulation (Fig. 3G). Taken together, these results indicate that PHZ did not inhibit the inflammatory response or protect the BMB *in vitro*.

3.4 Oral administration of PHZ regulates the composition of intestinal flora in mastitis mice

The involvement of intestinal flora in regulating mastitis has been established[20]. We investigated whether oral administration of PHZ regulates intestinal flora using 16S rRNA high-throughput sequencing to detect changes in the intestinal flora. OTU analysis of intestinal flora revealed that PHZ caused the emergence of different OTUs to NT group (Figs. S2A). *α*-Diversity analysis indicated that PHZ did not alter the species richness and diversity of intestinal flora in mastitis mice (Figs. S2B-E). However, PCoA, NMDS, and UPGMA analysis demonstrated that PHZ significantly changed the intestinal flora composition of mastitis mice (Figs. S2F-H).

Linear discriminant analysiseffect size (LEfSe) analysis was used to identify significant differences in intestinal flora between the 2 groups of mice. The results showed that oral administration of PHZ decreased the relative abundance of Bacteroides and increased the

relative abundance of *Lactobacillus* in the intestinal flora of mastitis mice (Figs. 4A, B, F-I). Moreover, the species distribution histogram at the species level displayed the different relative abundance of *Bacteroides* and *Lactobacillus* (Fig. 4E). The analysis of the species distribution histogram at the phylum level indicated that oral administration of PHZ increased the abundance ratio of Firmicutes to Bacteroidota (Figs. 4C and D). To determine whether these changes in intestinal flora affect the level of SCFAs metabolism, we measured the SCAFs content in the feces of mice. The results showed that PHZ significantly increased the contents of acetic and propionic acids but did not affect butyric and caproic acid levels in the feces of mastitis mice (Figs. 4J-M).

3.5 PHZ does not solely rely on regulating intestinal flora to improve mastitis.

To determine whether the protective effect of PHZ on mice mastitis depends on intestinal flora, we treated mice with an ABX to disrupt the intestinal flora (Fig. 5A). Even after disturbing the intestinal flora, PHZ significantly improved pathological symptoms,

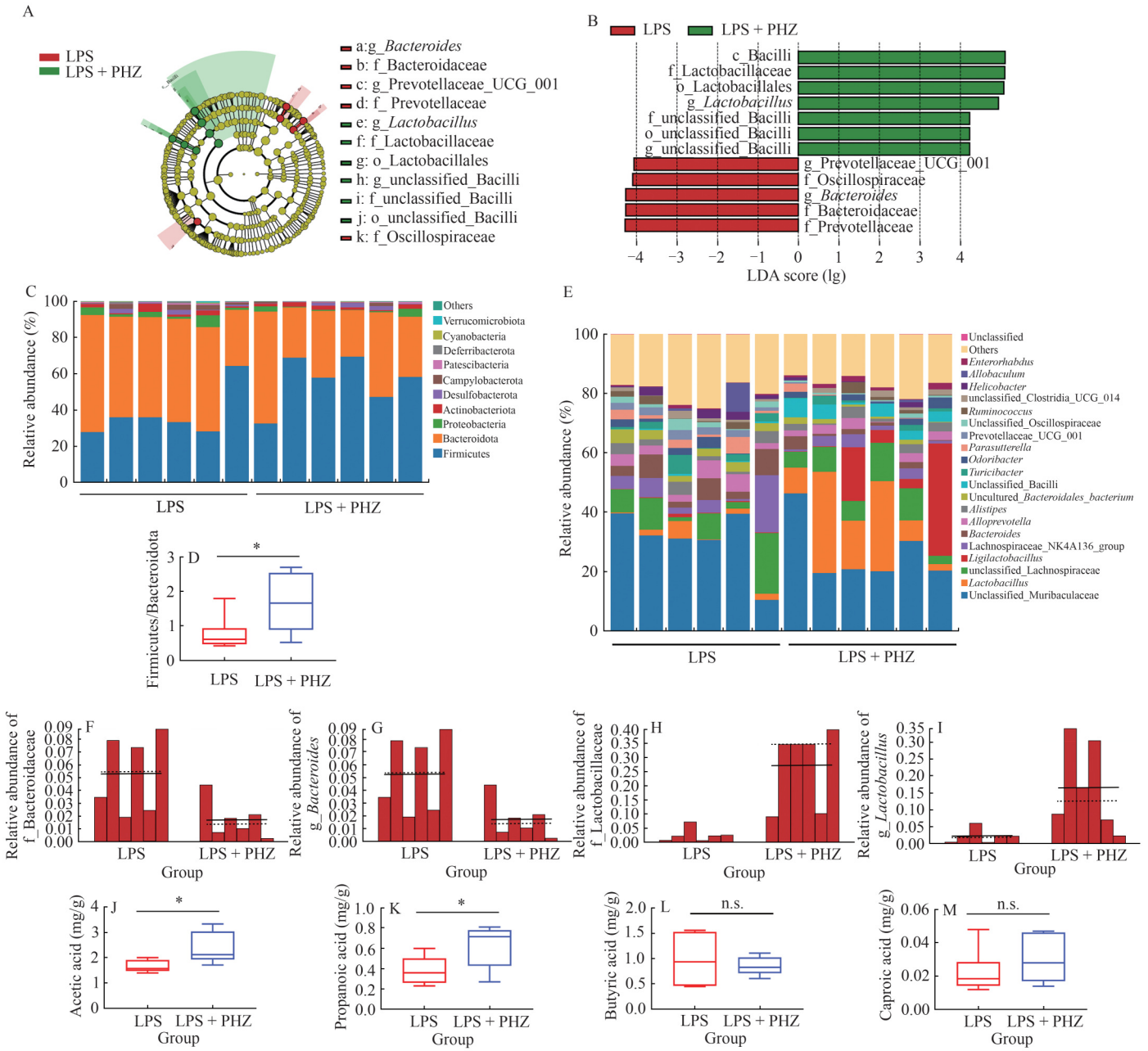

Fig. 4 Oral administration of PHZ regulates the composition of intestinal flora in mastitis mice. (A, B) LEfSe analysis of intergroup samples revealed differences in phylum to genus classification between the 2 groups (lg (LDA score) > 3). The analysis results are shown as LEfSe analysis of the evolutionary (A) branching diagram and (B) histogram of LDA value distribution. (C) Comparison of phylum abundance in the 2 groups. (D) Relative abundance ratio of Firmicutes to Bacteroidota. (E) Comparison of genus abundance in the 2 groups. Relative abundance of (F) Bacteroidaceae, (G) *Bacteroides*, (H) Lactobacillaceae, and (I) *Lactobacillus* in the 2 groups. Concentrations of (J) acetic, (K) propionic, (L) butyric, and (M) caproic acids in the feces of the 2 groups of mice. Data are presented as mean ± SD ($n = 6$). *$P < 0.05$; n.s. not significant.

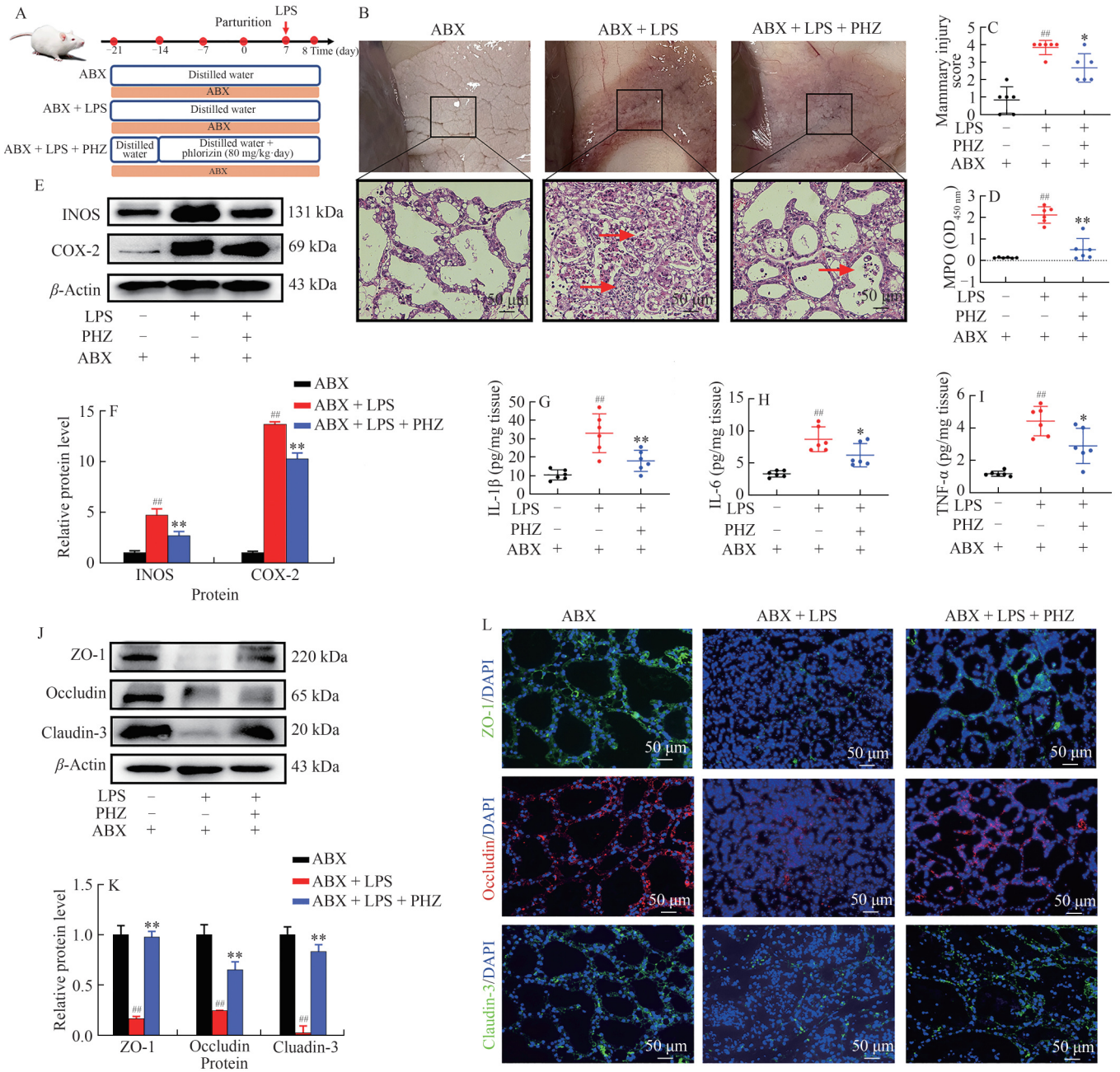

Fig. 5 PHZ does not solely rely on regulating intestinal flora to improve mastitis. (A) Timeline of the experimental procedure. (B) Representative photographs and H&E staining images of mouse mammary glands. The red arrows indicate inflammatory cell infiltration. Scale bar: 50 μm. (C) Mammary injury score based on H&E staining. (D) MPO levels in mammary glands. (E and F) Representative bands and relative protein levels of proinflammatory enzymes (INOS and COX-2). *β*-Actin was used as the internal control to obtain the relative protein intensity. Contents of proinflammatory factors (G) IL-1β, (H) IL-6, and (I) TNF-α in mouse mammary tissue. (J, K) Representative bands and relative protein levels of TJs (ZO-1, Occludin, and Claudin-3). (L) Representative images of the immunofluorescence of TJs (ZO-1, Occludin, and Claudin-3). Scale bar: 50 μm. Data are presented as mean ± SD ($n = 6$). $^{\#\#}P < 0.01$ *vs*. ABX group; $^{*}P < 0.05$ or $^{**}P < 0.01$ *vs*. ABX + LPS group.

such as mammary redness and inflammatory cell infiltration in mammary acini caused by LPS stimulation (Figs. 5B-D). Additionally, the detection of pro-inflammatory mediators revealed that the secretion of pro-inflammatory factors and enzymes in the mammary tissue of mice in the ABX + LPS + PHZ group was lower than that in the ABX + LPS group (Figs. 5E-I). The BMB analysis results demonstrated a significant decrease in the protein expression of TJs in the mammary glands of mice in the ABX + LPS group. PHZ administration significantly increased the expression of TJs in this group (Figs. 5J-L). Consistent with these findings, the activity of the NF-κB signaling pathway, NLRP3 inflammasome, and GSDMD were significantly decreased in the ABX + LPS + PHZ group compared with that in the ABX + LPS group (Figs. S3A-G). These results suggest that the inhibitory effect of PHZ on mastitis and its protective effect on BMB do not solely depend on regulating intestinal flora, implying that PHZ may improve mastitis by metabolizing to other substances.

3.6 PHZ inhibits pyroptosis and protects the BMB by metabolizing into PHT

Based on the aforementioned results, we speculated that PHZ may undergo metabolism in the body to produce other active ingredients, contributing to its anti-inflammatory function. Therefore, we determined the levels of PHZ and its metabolite PHT in the blood of mastitis mice. The results demonstrated that PHZ was barely detectable in the serum of mice in LPS + PHZ and ABX + LPS + PHZ groups, whereas PHT levels increased significantly (Figs. 6A and S4A). Based on the

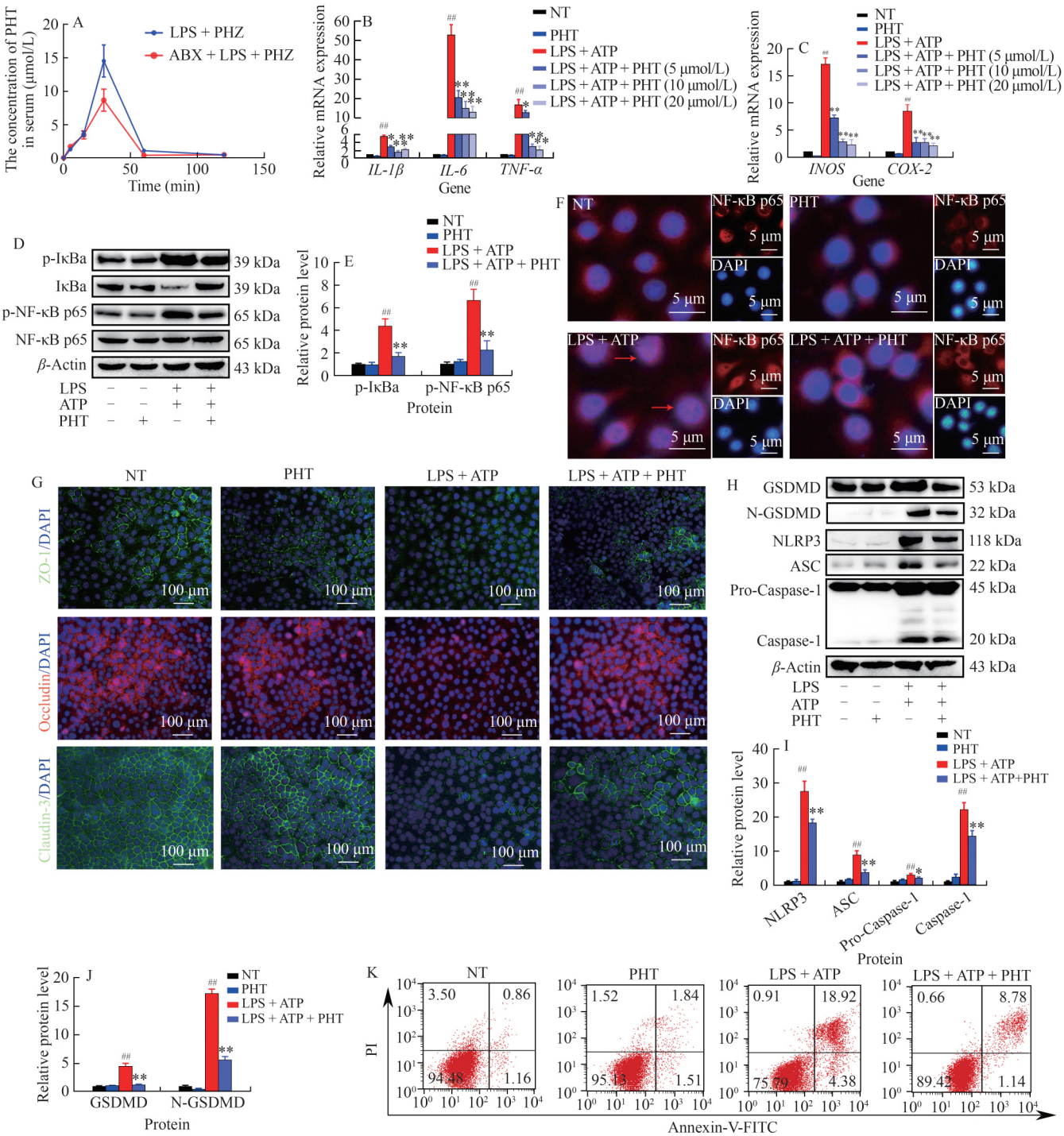

Fig. 6 PHZ inhibits pyroptosis and protects the BMB by metabolizing into PHT. (A) Plasma concentration-time profile of PHT in mice. After treating mMECs with PHT for 1 h, they were stimulated with LPS (1 μg/mL) for 4 or 24 h, and ATP (5 mmol/L) co-stimulation was introduced either 30 or 90 min before the completion of LPS stimulation. (B) Relative mRNA expression of proinflammatory factors. (C) Relative mRNA expression of pro-inflammatory enzymes. (D) Representative bands of p-IκB, IκB, p-NF-κB p65, and NF-κB p6. (E) Relative protein levels of p-IκB and p-NF-κB p65. (F) Nuclear translocation of NF-κB p65 of mMECs under different treatments. Scale bar: 5 μm. (G) Representative images of the immunofluorescence of TJs. Scale bar: 100 μm. (H) Representative bands and (I, J) relative protein levels of NLRP3, ASC, pro-Caspase-1, Caspase-1, GSDMD, and N-GSDMD. (K) Determination of cell pyroptosis using flow cytometry. Data are presented as mean ± SD ($n = 3$). $^{\#\#}P < 0.01$ *vs*. NT group; $^{*}P < 0.05$ or $^{**}P < 0.01$ *vs*. LPS + ATP group; n.s. not significant.

PHT concentration in mouse blood, we selected 5, 10, and 20 μmol/L PHT to investigate its anti-inflammatory effect. Above all, our resulted showed PHT did not affect the mMEC viability at concentrations below 50 μmol/L (Fig. S4B). The results indicated that PHT dose-dependently reduced the overexpression of pro-inflammatory factors and enzymes in LPS + ATP-stimulated mMECs (Figs. 6B and C). The 10 μmol/L PHT was selected for subsequent experiments. In LPS + ATP stimulated mMECs, PHT significantly inhibited the phosphorylation of IκB and NF-κB p65, leading to reduced nuclear translocation of NF-κB p65 (Figs. 6D-F). Further investigation revealed that PHT significantly ameliorated the loss of TJs in LPS + ATP-stimulated mMECs (Figs. 6G and S4C-D). Concurrently, PHT effectively suppressed the activation of the NLRP3 inflammasome (Figs. 6H and I). Notably, PHT significantly improved cell survival, reduced the increase in GSDMD levels and cleavage, and prevented pyroptosis in LPS + ATP-stimulated mMECs (Figs. 6K, J and S4E-G).

3.7 PHT inhibits pyroptosis and protects the BMB via autophagy activation.

Pyroptosis is regulated by autophagy via a variety of methods. The effect of PHT on autophagy in LPS-stimulated mMECs was investigated. PHT was observed to significantly increase the expression of LC3 II while decreasing the expression of p62 in LPS + ATP-stimulated mMECs (Figs. 7A and B). Moreover, the results revealed that PHT significantly induced autolysosome formation, whereas LPS + ATP-stimulation hindered the formation of autophagosomes and autolysosomes. Notably, a higher number of autophagosomes and autolysosomes was

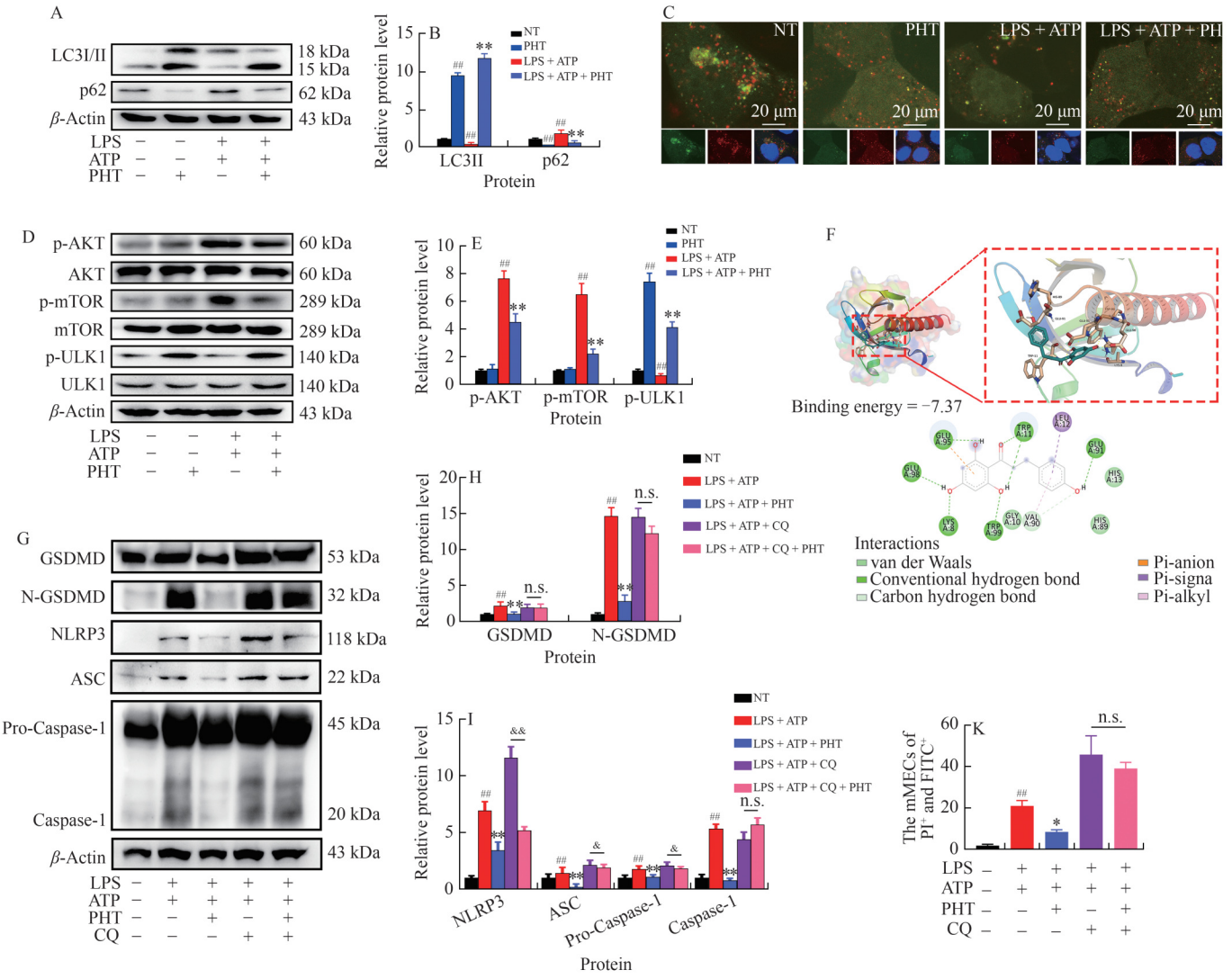

Fig. 7 PHT inhibits pyroptosis and protects the BMB *via* autophagy activation. After treating mMECs with PHT (10 μmol/L) for 1 h, they were stimulated with LPS (1 μg/mL) for 1 h, and ATP (5 mmol/L) co-stimulation was introduced 30 min before the completion of LPS stimulation. (A, B) Representative bands and relative protein levels of LC3 I/II and p62 in mMECs. (C) Confocal image of successfully transfected mMECs with mRFP-GFP-LC3 plasmid. Scale bar: 20 μm. (D) Representative bands of p-AKT, AKT, p-mTOR, TOR, p-ULK1, and ULK1 in mMECs. (E) Relative protein levels of p-AKT, p-mTOR, and p-ULK1 in mMECs. (F) Virtual docking of PHT and AKT protein. After pretreatment of mMECs with CQ (50 μmol/L) for 1 h, they were treated with PHT (10 μmol/L) for 1 h, followed by LPS (1 μg/mL) stimulation for 1, 4, or 24 h. ATP (5 mmol/L) was added for co-stimulation 30 or 90 min before the completion of LPS stimulation. (G-I) Representative bands and relative protein level of NLRP3, ASC, pro-Caspase-1, Caspase-1, GSDMD, and N-GSDMD. (K and J) Determination of cell pyroptosis using flow cytometry. Data are presented as mean ± SD ($n = 3$). $^{\#\#}P < 0.01$ *vs.* NT group; $^{**}P < 0.01$ *vs.* LPS + ATP group; $^{\&}P < 0.05$ or $^{\&\&}P < 0.01$ *vs.* LPS + ATP + CQ group.

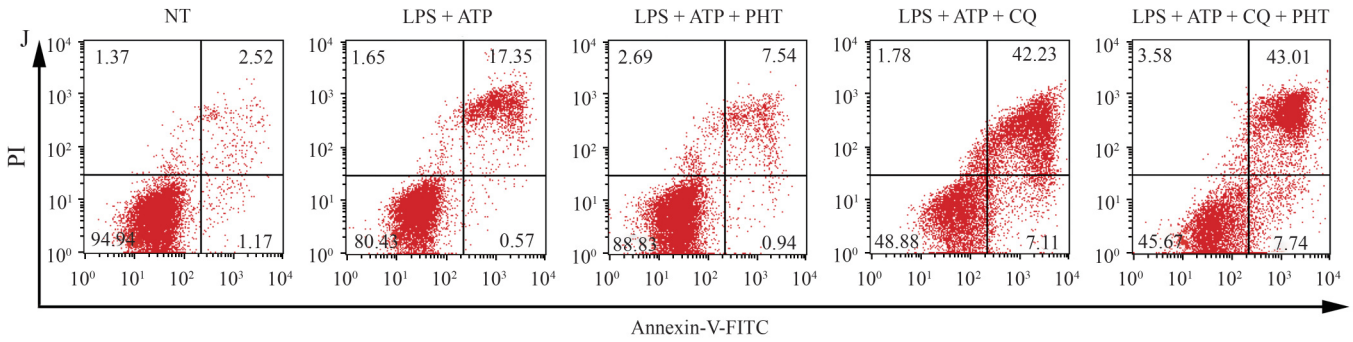

Fig. 7 (*continued*)

detected in mMECs co-treated with PHT and LPS + ATP than in those stimulated with LPS + ATP alone (Fig. 7C). Additionally, the results showed PHT significantly inhibited AKT/mTOR phosphorylation and increase ULK1 phosphorylation in LPS + ATP-stimulated mMECs (Figs. 7D and E). Virtual docking between PHT and AKT protein revealed conventional hydrogen and carbon-hydrogen bonds formed at multiple amino acid residues of AKT protein, with a binding energy of < –7.0 kcal/mol (Fig. 7I). This observation suggests that PHT may inhibit AKT phosphorylation by binding to AKT protein. Furthermore, autophagy in mammary tissue was examined, and the trends observed in LC3 II and p62 levels were consistent with the *in vitro* results. Oral administration of PHZ significantly enhanced autophagy (Figs. S5A and B). Additionally, the oral administration of PHZ in mice inhibited AKT/mTOR phosphorylation and increased ULK1 phosphorylation in mammary tissue (Figs. S5C and D).

To investigate this further, we conducted follow-up studies using the autophagy inhibitor chloroquine (CQ). The results confirmed the significant inhibitory effect of CQ on autophagy (Figs. S6A and B). Subsequently, the results revealed that CQ did not affect the inhibition of PHT on the NF-κB signaling pathway (Figs. S6C and D). Moreover, CQ did not alter the inhibitory effects of PHT on the protein expression of NLRP3, ASC, and pro-Caspase-1 in LPS + ATP-stimulated mMECs. However, CQ reversed the inhibitory effect of PHT on the activation of NLRP3 inflammasome, as evidenced by the protein expression of Caspase-1 (Figs. 7G and I). Additionally, CQ reversed the inhibitory effects of PHT on LPS + ATP-stimulated pyroptosis of mMECs, as observed through the cleavage of GSDMD and an increase in the number of PI/FITC double-positive cells (Figs. 7G, H, K and J). The results of TJs detection were consistent with those of the pyroptosis assay. Particularly, CQ significantly reversed the protective effect of PHT on the BMB (Figs. S6E and F). These results suggest that PHT inhibits the activation of the NLRP3 inflammasome by activating autophagy, thereby improving pyroptosis and protecting the BMB.

4. Discussion

In this study, we demonstrated that oral administration of PHZ alleviated LPS-induced mastitis and protected the BMB while reducing the occurrence of pyroptosis within the mouse mammary gland. The potential mechanism involved the *in vivo* metabolism of PHZ into PHT, wherein PHT inhibited the activation of the NLRP3 inflammasome by activating autophagy, hence mitigating pyroptosis. Additionally, we demonstrated that oral administration of PHT regulated the intestinal flora to encourage SCFA production, which also is one of the mechanisms by which PHT inhibits inflammation.

Intense inflammation and the breakdown of the BMB in the mammary gland are the main pathological characteristics of mastitis, an inflammatory disease that commonly affects mammals lactating[22]. Pyroptosis is a recently discovered form of programmed cell death (PCD) that occurs more rapidly than other PCDs and is accompanied by the release of pro-inflammatory factors, such as IL-1β. The involvement of pyroptosis in a wide range of inflammation-related diseases, such as neurodegenerative disorders, inflammatory bowel disease (IBD), and acute lung injury (ALI), has been repeatedly demonstrated by research[23-25]. Studies by Zuo et al.[26] and Wang et al.[27] demonstrated that pyroptosis of mammary epithelial cells played a key role in the aggravation of mastitis. Our study results showed that oral administration of PHZ significantly improved the inflammatory response of the mammary gland and the breakdown of the BMB in mice with LPS-induced mastitis. Moreover, it reduced the activation of the pyroptosis executive protein-GSDMD. Activation of the NLRP3 inflammasome is a classical pathway for the occurrence of pyroptosis. The appearance of Caspase-1 with zymogenic activity directly induces the cleavage of GSDMD and releases the N-terminal domain to perform pyroptosis[28]. Meanwhile, the NF-κB signaling pathway affects the occurrence of pyroptosis by regulating the transcription of NLRP3 inflammasome component proteins (NLRP3, ASC, and Caspase-1) and GSDMD[29]. Our study results showed that oral administration of PHZ significantly inhibited the activation of NLRP3 inflammasome and NF-κB in the mammary tissue of mastitis mice. However, our findings demonstrated that PHZ was not anti-inflammatory and protective of the BMB *in vitro*. In LPS + ATP-stimulated mMECs, PHZ had no discernible influence on pyroptosis, NLRP3 inflammasome activation, or the NF-κB signaling pathway.

Intestinal flora has been established to exhibit immunomodulatory functions in several studies. It affects the pathological reactions of distal organs by regulating the metabolism of SCFAs, tryptophan, and bile acids. Based on this, the concepts of gut-liver, gut-brain, and gut-lung axes have been proposed successively[30-32]. The involvement of intestinal flora in the occurrence and development of mastitis has led to the proposal of the "gut-milk axis" concept. Zhao et al.[33-34] demonstrated that it is possible to treat mastitis by controlling the intestinal flora's metabolism of tryptophan and SCFAs through diet. PHZ reportedly exerts antioxidant functions and improves insulin resistance by targeting gut microbiota to increase SCFA production[35-36]. Therefore, based on the difference between the results of PHZ *in vivo* and *in vitro*, we speculated that PHZ might exert its anti-inflammatory

effect by regulating intestinal flora. Our results showed that the abundance of *Bacteroides* in the intestinal flora of mastitis mice decreased, and the abundance of *Lactobacillus* increased significantly after oral administration of PHZ in mastitis mice. Meanwhile, the contents of acetic and propionic acids increased, but butyric and caproic acid levels were not different in mouse feces. Our study showed that oral administration of PHZ did not affect the content of butyric acid, which differents with the findings of Zhang et al.[36]. This discrepancy could be attributed to differences in the duration of oral administration of PHZ. To determine whether the effect of PHZ on mastitis depends on the intestinal flora, we used ABX to disrupt intestinal flora. Even after upsetting the intestinal flora, the impact of PHZ on mastitis was still noticeable. Therefore, we hypothesized that although oral administration of PHZ has a prebiotic function of regulating intestinal flora and increasing SCFA production, this is not the main mechanism by which it improves mastitis.

Research has shown that in both oral and intravenous administrations of PHZ in rats, the major existing forms of PHZ in the blood were its metabolite PHT[21]. Moreover, Chang et al.[37] evaluated the anti-inflammatory effects of PHT and PHZ in LPS-stimulated RAW264.7 cells, and their results showed that PHT had anti-inflammatory effects while PHZ did not. Additionally, the inhibitory effect of PHZ on the NLRP3 inflammasome has been reported in several studies[38-39]. Combining previous study findings with our results, we hypothesized that PHZ may be metabolized to PHT to perform the anti-inflammatory function *in vivo*. In our study, PHT was detected in the blood of mastitis mice after oral administration of PHZ. However, the time-concentration curves of PHT correlated with previous studies were not the same, possibly owing to species differences between rats and mice. The evident anti-inflammatory, anti-pyroptosis, and BMB protecting properties of PHT *in vitro* were supported by our studies. These findings indicate that the anti-inflammatory effect of oral administration of PHZ is primarily achieved by metabolizing into PHT *in vivo*.

The studies of Chhimwal et al.[40] demonstrated that PHT reduced oxidative damage and inflammatory response by regulating autophagy. Our results suggested that PHT significantly promoted autophagy and enhanced autophagy flux in LPS + ATP-stimulated mMECs. Further results of autophagy-related signaling pathways were consistent with those of previous studies. PHT decreased the phosphorylation of AKT and mTOR and promoted the phosphorylation of ULK1[41]. Moreover, virtual docking showed that PHT may possess binding sites with AKT protein, potentially explaining its inhibitory effect on AKT phosphorylation. However, this conclusion needs further experimental verification. Autophagy has the ability to inhibit the NF-κB signaling pathway and NLRP3 inflammasome activation in inflammation-related conditions[42-43]. In this study, PHT inhibited the activation of NLRP3 inflammasome through autophagy, thus reducing the occurrence of pyroptosis. However, the inhibitory effect of PHT on the NF-κB signaling pathway does not involve the activation of autophagy. PHT mediates the degradation of Keap1 by activating autophagy and then promotes the activation of Nrf2[44]. As a crucial antioxidant signal, Nrf2 is involved in eliminating intracellular reactive oxygen species, which act as catalysts for the activation of the NLRP3 inflammasome[45]. Furthermore, by stopping damaged mitochondria from releasing DAMPs, mitochondrial autophagy effectively inhibits the overactivation of the NLRP3 inflammasome[46]. These mechanisms might explain how PHT activates autophagy to specifically inhibit the activation of the NLRP3 inflammasome, and this will be a crucial area of focus for our subsequent research.

In conclusion, our research demonstrated that PHZ does not possess an independent anti-inflammatory effect; instead, it reduces inflammation *in vivo* by metabolizing into PHT. However, oral administration of PHZ displays prebiotic effects by increasing the abundance of *Lactobacillus* and levels of SCFAs (Fig. 8). Therefore, consuming apples regularly to maintain nutrient intake, such as PHT, could represent a potential approach to prevent mastitis during lactation.

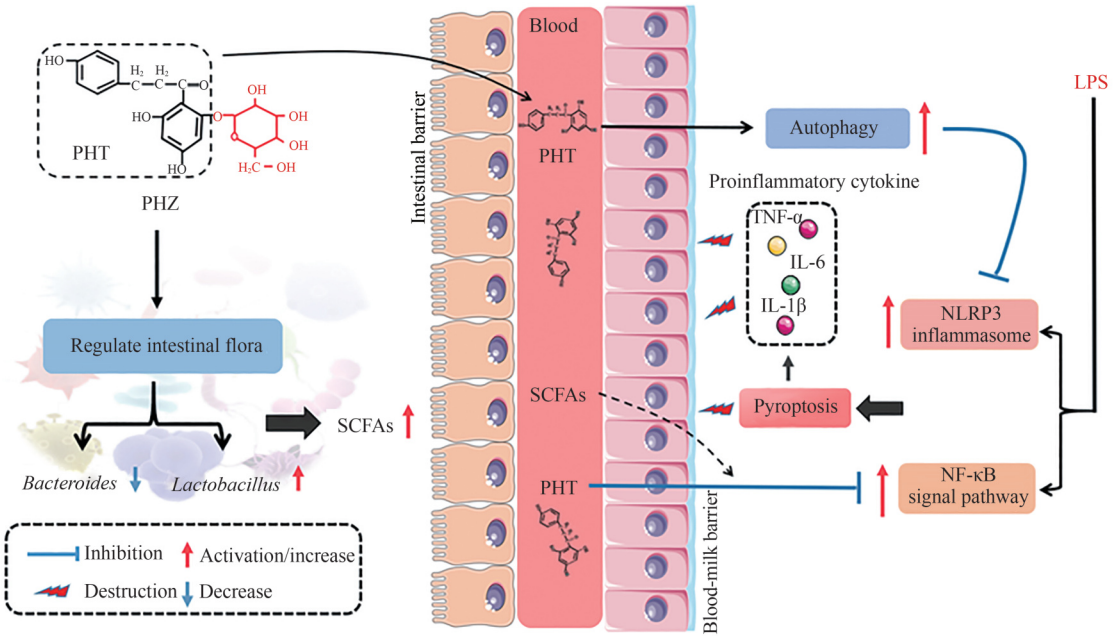

Fig. 8 Mechanism of PHZ in alleviating LPS-induced mice mastitis. Oral administration of PHZ alleviated LPS-induced mastitis and protected the BMB. The potential mechanism involved the *in vivo* metabolism of PHZ into PHT, wherein PHT inhibited the activation of the NLRP3 inflammasome by activating autophagy, consequently alleviating pyroptosis. Additionally, oral administration of PHZ regulated the intestinal flora to encourage SCFA production, which also is one of the mechanisms by which PHZ inhibits inflammation.

Disclosure of conflicts of interest

The authors declare that they have no competing interests.

Acknowledgements

National Natural Science Foundation of China (32272955, 32172807).

Data Availability Statement

All relevant data about this research can be requested from the corresponding author.

Appendix A. Supplementary data

Supplementary data associated with this article can be found, in the online version, at http://doi.org/10.26599/FSHW.2024.9250147.

Reference

[1] C.H. Lin, P.R. Yang, C.P. Lee, et al., Descriptive study of mastitis in postpartum women in Taiwan: incidence and related factors, J. Womens Health (Larchmt) 32 (2023) 616-622. https://doi.org/10.1089/jwh.2022.0303.

[2] Z. Yu, S. Sun, Y. Zhang, High-Risk factors for suppurative mastitis in lactating women, Med. Sci. Monit. 24 (2018) 4192-4197. https://doi.org/10.12659/MSM.909394.

[3] A. Ujita, H. Ryu, H. Kobayashi, et al., Pneumococcal lactational mastitis in a healthy woman, BMJ Case Rep. 15 (2022) 250277. https://doi.org/10.1136/bcr-2022-250277.

[4] S. Xu, Q. Yu, Bacterial factors of mastitis in lactating women and its effect on the physical properties and chemical composition of breast milk, Cell Mol. Biol. 67 (2021) 172-177. https://doi.org/10.14715/cmb/2021.67.3.27.

[5] T.M. Samuel, C.A. de Castro, S. Dubascoux, et al., Subclinical mastitis in a European multicenter cohort: prevalence, impact on human milk (HM) composition, and association with infant HM intake and growth, Nutrients 12 (2019) 105. https://doi.org/10.3390/nu12010105.

[6] Y. Tsugami, K. Matsunaga, T. Suzuki, et al., Phytoestrogens weaken the blood-milk barrier in lactating mammary epithelial cells by affecting tight junctions and cell viability, J. Agric. Food Chem. 65 (2017) 11118-11124. https://doi.org/10.1021/acs.jafc.7b04786.

[7] C. Li, X. Wang, M. Kuang, et al., UFL1 modulates NLRP3 inflammasome activation and protects against pyroptosis in LPS-stimulated bovine mammary epithelial cells, Mol. Immunol. 112 (2019) 1-9. https://doi.org/10.1016/j.molimm.2019.04.023.

[8] Y. Wu, J. Zhang, S. Yu, et al., Cell pyroptosis in health and inflammatory diseases, Cell Death Discov. 8 (2022) 191. https://doi.org/10.1038/s41420-022-00998-3.

[9] T. Xu, Z. Dong, X. Wang, et al., IL-1β induces increased tight junction permeability in bovine mammary epithelial cells *via* the IL-1β-ERK1/2-MLCK axis upon blood-milk barrier damage, J. Cell Biochem. 119 (2018) 9028-9041. https://doi.org/10.1002/jcb.27160.

[10] M.C. Afeiche, A. Iroz, F. Thielecke, et al., The dietary inflammatory index is associated with subclinical mastitis in lactating European women, Nutrients 14 (2022) 4719. https://doi.org/10.3390/nu14224719.

[11] J.H. Martin, S. Crotty, P. Warren, et al., Does an apple a day keep the doctor away because a phytoestrogen a day keeps the virus at bay? a review of the anti-viral properties of phytoestrogens, Phytochemistry 68 (2007) 266-274. https://doi.org/10.1016/j.phytochem.2006.11.018.

[12] A. Suarez-Jacobo, C.E. Rufer, R. Gervilla, et al., Influence of ultra-high pressure homogenisation on antioxidant capacity, polyphenol and vitamin content of clear apple juice, Food Chem. 127 (2011) 447-454. https://doi.org/10.1016/j.foodchem.2010.12.152.

[13] D. Barreca, E. Bellocco, G. Lagana, et al., Biochemical and antimicrobial activity of phloretin and its glycosilated derivatives present in apple and kumquat, Food Chem. 160 (2014) 292-297. https://doi.org/10.1016/j.foodchem.2014.03.118.

[14] J.R. Ehrenkranz, N.G. Lewis, C.R. Kahn, et al., Phlorizin: a review, Diabetes Metab. Res. Rev. 21 (2005) 31-38. https://doi.org/10.1002/dmrr.532.

[15] C. Ghezzi, D.D.F. Loo, E.M. Wright, Physiology of renal glucose handling via SGLT1, SGLT2 and GLUT2, Diabetologia 61 (2018) 2087-2097. https://doi.org/10.1007/s00125-018-4656-5.

[16] X. Mei, X. Zhang, Z. Wang, et al., Insulin sensitivity-enhancing activity of phlorizin is associated with lipopolysaccharide decrease and gut microbiota changes in obese and type 2 diabetes (*db*/*db*) mice, J. Agric. Food Chem. 64 (2016) 7502-7511. https://doi.org/10.1021/acs.jafc.6b03474.

[17] S.P. Kamdi, A. Raval, K.T. Nakhate, Phloridzin attenuates lipopolysaccharide-induced cognitive impairment *via* antioxidant, anti-inflammatory and neuromodulatory activities, Cytokine 139 (2021) 155408. https://doi.org/10.1016/j.cyto.2020.155408.

[18] L. Cardoso-Sousa, E.M.G. Aguiar, D.C. Caixeta, et al., Effects of salbutamol and phlorizin on acute pulmonary inflammation and disease severity in experimental sepsis, PLoS One 14 (2019) e0222575. https://doi.org/10.1371/journal.pone.0222575.

[19] X. Ran, J. Liu, S. Fu, et al., Phytic acid maintains the integrity of the blood-milk barrier by regulating inflammatory response and intestinal flora structure, J. Agric. Food Chem. 70 (2022) 381-391. https://doi.org/10.1021/acs.jafc.1c06270.

[20] X.Y. Hu, J. Guo, C.J. Zhao, et al., The gut microbiota contributes to the development of *Staphylococcus aureus*-induced mastitis in mice, ISME Journal 14 (2020) 1897-1910. https://doi.org/10.1038/s41396-020-0651-1.

[21] Z. Wang, Z. Gao, A. Wang, et al., Comparative oral and intravenous pharmacokinetics of phlorizin in rats having type 2 diabetes and in normal rats based on phase II metabolism, Food Funct. 10 (2019) 1582-1594. https://doi.org/10.1039/c8fo02242a.

[22] W. Guo, W. Li, Y. Su, et al., GPR109A alleviate mastitis and enhances the blood milk barrier by activating AMPK/Nrf2 and autophagy, Int. J. Biol. Sci. 17 (2021) 4271-4284. https://doi.org/10.7150/ijbs.62380.

[23] Q. Zhang, X.M. Huang, J. X. Liao, et al., LncRNA HOTAIR promotes neuronal damage through facilitating NLRP3 mediated-pyroptosis activation in Parkinson's disease via regulation of miR-326/ELAVL1 axis, Cell Mol. Neurobiol. 41 (2021) 1773-1786. https://doi.org/10.1007/s10571-020-00946-8.

[24] Z. Pu, B. Sui, X. Wang, et al., The effects and mechanisms of the anti-COVID-19 traditional Chinese medicine, Dehydroandrographolide from *Andrographis paniculata* (Burm.f.) Wall, on acute lung injury by the inhibition of NLRP3-mediated pyroptosis, Phytomedicine 114 (2023) 154753. https://doi.org/10.1016/j.phymed.2023.154753.

[25] Q. Liang, W. Cai, Y. Zhao, et al., Lycorine ameliorates bleomycin-induced pulmonary fibrosis *via* inhibiting NLRP3 inflammasome activation and pyroptosis, Pharmacol. Res. 158 (2020) 104884. https://doi.org/10.1016/j.phrs.2020.104884.

[26] X.M. Zuo, T.S. Wang, X.G. Shi, et al., Pyroptosis: the pathological process that dominates granulomatous lobular mastitis, J. Physiol. Pharmacol. 72 (2021) 15. https://doi.org/10.26402/jpp.2021.3.15.

[27] X.Z. Wang, M.C. Liu, N. Geng, et al., *Staphylococcus aureus* mediates pyroptosis in bovine mammary epithelial cell via activation of NLRP3 inflammasome, Vet. Res. 53 (2022) 10. https://doi.org/10.1186/s13567-022-01027-y.

[28] R.C. Coll, K. Schroder, P. Pelegrin, NLRP3 and pyroptosis blockers for treating inflammatory diseases, Trends Pharmacol. Sci. 43 (2022) 653-668. https://doi.org/10.1016/j.tips.2022.04.003.

[29] Z. Liu, L. Gan, Y. Xu, et al., Melatonin alleviates inflammasome-induced pyroptosis through inhibiting NF-kappaB/GSDMD signal in mice adipose tissue, J. Pineal. Res. 63 (2017) 12414. https://doi.org/10.1111/jpi.12414.

[30] Z.J. Wang, J. Liu, F. Li, et al., The gut-lung axis in severe acute *Pancreatitis*-associated lung injury: the protection by the gut microbiota through short-chain fatty acids, Pharmacol. Res. 182 (2022) 106321. https://doi.org/10.1016/j.phrs.2022.106321.

[31] C. Chen, J. Liao, Y. Xia, et al., Gut microbiota regulate Alzheimer's disease pathologies and cognitive disorders via PUFA-associated neuroinflammation, Gut 71 (2022) 2233-2252. https://doi.org/10.1136/gutjnl-2021-326269.

[32] H. Tilg, T.E. Adolph, M. Trauner, Gut-liver axis: pathophysiological concepts and clinical implications, Cell Metab. 34 (2022) 1700-1718. https://doi.org/10.1016/j.cmet.2022.09.017.

[33] C. Zhao, X. Hu, L. Bao, et al., Aryl hydrocarbon receptor activation by *Lactobacillus reuteri* tryptophan metabolism alleviates *Escherichia coli*-induced

mastitis in mice, PLoS Pathog. 17 (2021) e1009774. https://doi.org/10.1371/journal.ppat.1009774.

[34] C. Zhao, L. Bao, Y. Zhao, et al., A fiber-enriched diet alleviates *Staphylococcus aureus*-induced mastitis by activating the HDAC3-mediated antimicrobial program in macrophages *via* butyrate production in mice, PLoS Pathog. 19 (2023) e1011108. https://doi.org/10.1371/journal.ppat.1011108.

[35] D. Liu, Y. Ji, Y. Guo, et al., Dietary supplementation of apple phlorizin attenuates the redox state related to gut microbiota homeostasis in C57BL/6J mice fed with a high-fat diet, J. Agric. Food Chem. 69 (2021) 198-211. https://doi.org/10.1021/acs.jafc.0c06426.

[36] X.Y. Zhang, J. Chen, K. Yi, et al., Phlorizin ameliorates obesity-associated endotoxemia and insulin resistance in high-fat diet-fed mice by targeting the gut microbiota and intestinal barrier integrity, Gut Microbes 12 (2020) 1-18. https://doi.org/10.1080/19490976.2020.1842990.

[37] W.T. Chang, W. C. Huang, C.J. Liou, Evaluation of the anti-inflammatory effects of phloretin and phlorizin in lipopolysaccharide-stimulated mouse macrophages, Food Chem. 134 (2012) 972-979. https://doi.org/10.1016/j.foodchem.2012.03.002.

[38] D. Cui, S. Liu, M. Tang, et al., Phloretin ameliorates hyperuricemia-induced chronic renal dysfunction through inhibiting NLRP3 inflammasome and uric acid reabsorption, Phytomedicine 66 (2020) 153111. https://doi.org/10.1016/j.phymed.2019.153111.

[39] M. Wu, P. Li, Y. An, et al., Phloretin ameliorates dextran sulfate sodium-induced ulcerative colitis in mice by regulating the gut microbiota, Pharmacol. Res. 150 (2019) 104489. https://doi.org/10.1016/j.phrs.2019.104489.

[40] J. Chhimwal, A. Goel, M. Sukapaka, et al., Phloretin mitigates oxidative injury, inflammation, and fibrogenic responses via restoration of autophagic flux in *in vitro* and preclinical models of NAFLD, J. Nutr. Biochem. 107 (2022) 109062. https://doi.org/10.1016/j.jnutbio.2022.109062.

[41] C. Fan, Y. Zhang, Y. Tian, et al., Phloretin enhances autophagy by impairing AKT activation and inducing JNK-Beclin-1 pathway activation, Exp. Mol. Pathol. 127 (2022) 104814. https://doi.org/10.1016/j.yexmp.2022.104814.

[42] Q. Di, X. Zhao, H. Tang, et al., USP22 suppresses the NLRP3 inflammasome by degrading NLRP3 *via* ATG5-dependent autophagy, Autophagy 19 (2023) 873-885. https://doi.org/10.1080/15548627.2022.2107314.

[43] R. Lu, Z. Wei, Z. Wang, et al., Mulberroside A alleviates osteoarthritis via restoring impaired autophagy and suppressing MAPK/NF-kappaB/PI3K-AKT-mTOR signaling pathways, iScience 26 (2023) 105936. https://doi.org/10.1016/j.isci.2023.105936.

[44] T. Dierckx, M. Haidar, E. Grajchen, et al., Phloretin suppresses neuroinflammation by autophagy-mediated Nrf2 activation in macrophages, J. Neuroinflammation 18 (2021) 148. https://doi.org/10.1186/s12974-021-02194-z.

[45] J.Y. Kang, M.M. Xu, Y. Sun, et al., Melatonin attenuates LPS-induced pyroptosis in acute lung injury by inhibiting NLRP3-GSDMD pathway *via* activating Nrf2/HO-1 signaling axis, Int Immunopharmacol 109 (2022) 108782. https://doi.org/10.1016/j.intimp.2022.108782.

[46] M.J. Kim, J.H. Yoon, J.H. Ryu, Mitophagy: a balance regulator of NLRP3 inflammasome activation, BMB Rep. 49 (2016) 529-535. https://doi.org/10.5483/bmbrep.2016.49.10.115.